Figure S1

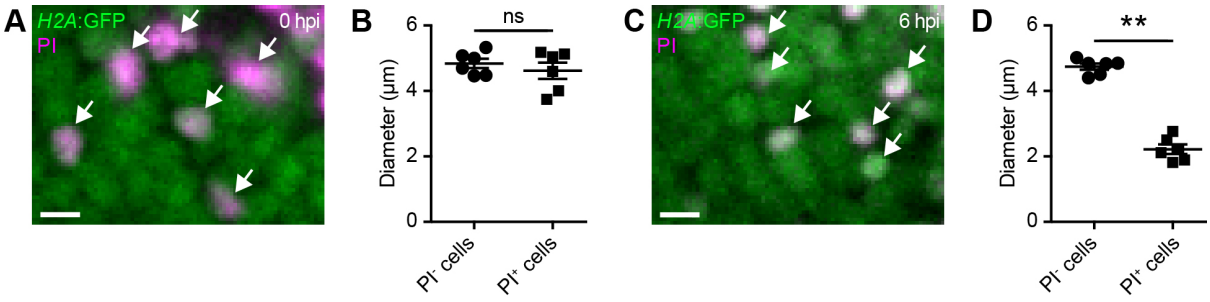

Figure S1. PI$^+$ cells are pyknotic at 6 hpi but not at 0 hpi. (A,C) Confocal images of PI$^+$ cells (white arrows) in *H2A*:GFP animals at 0 hpi (A) and 6 hpi (C). Scale bars, 5 µm. (B,D) Quantification of the size of PI$^-$ and PI$^+$ cells at 0 hpi (B) and 6 hpi (D). n = 6 animals per experimental group. ns, not significant and **, $p < 0.01$ in Mann-Whitney test.

Figure S2

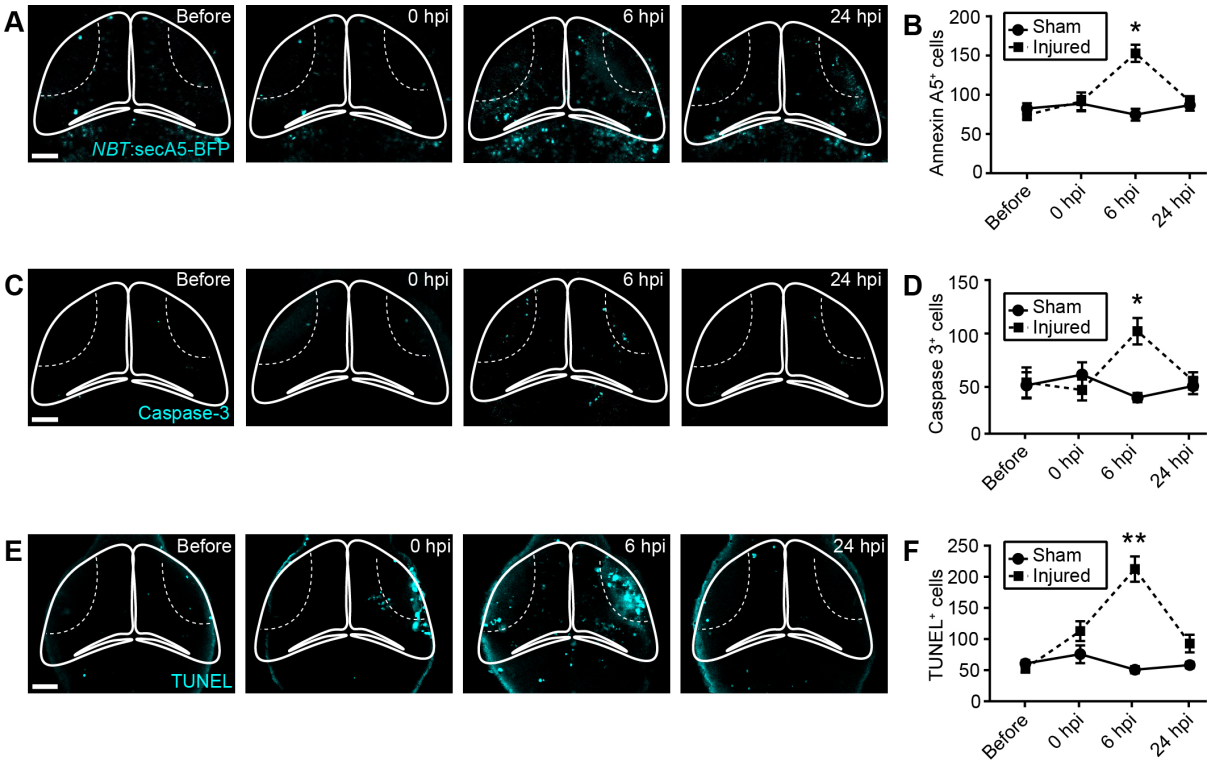

Fig. S2. Cell death after brain injury can be detected through Annexin A5 live imaging, caspase 3 immunohistochemistry, and TUNEL staining. (A,C,E) Confocal images of the tectum of a *NBT*:secA5-BFP animal (A), and animals after cleaved caspase 3 immunohistochemistry (B) or TUNEL staining (C), at different time points after injury. Scale bars, 50 µm. (B,D,F) Quantification of Annexin A5^{+} cells (B), cleaved caspase 3^{+} cells (D) or TUNEL^{+} cells (F). n ≥ 6 animals per experimental group. *, $p < 0.05$ and **, $p<0.01$ in two-way ANOVA.

Figure S3

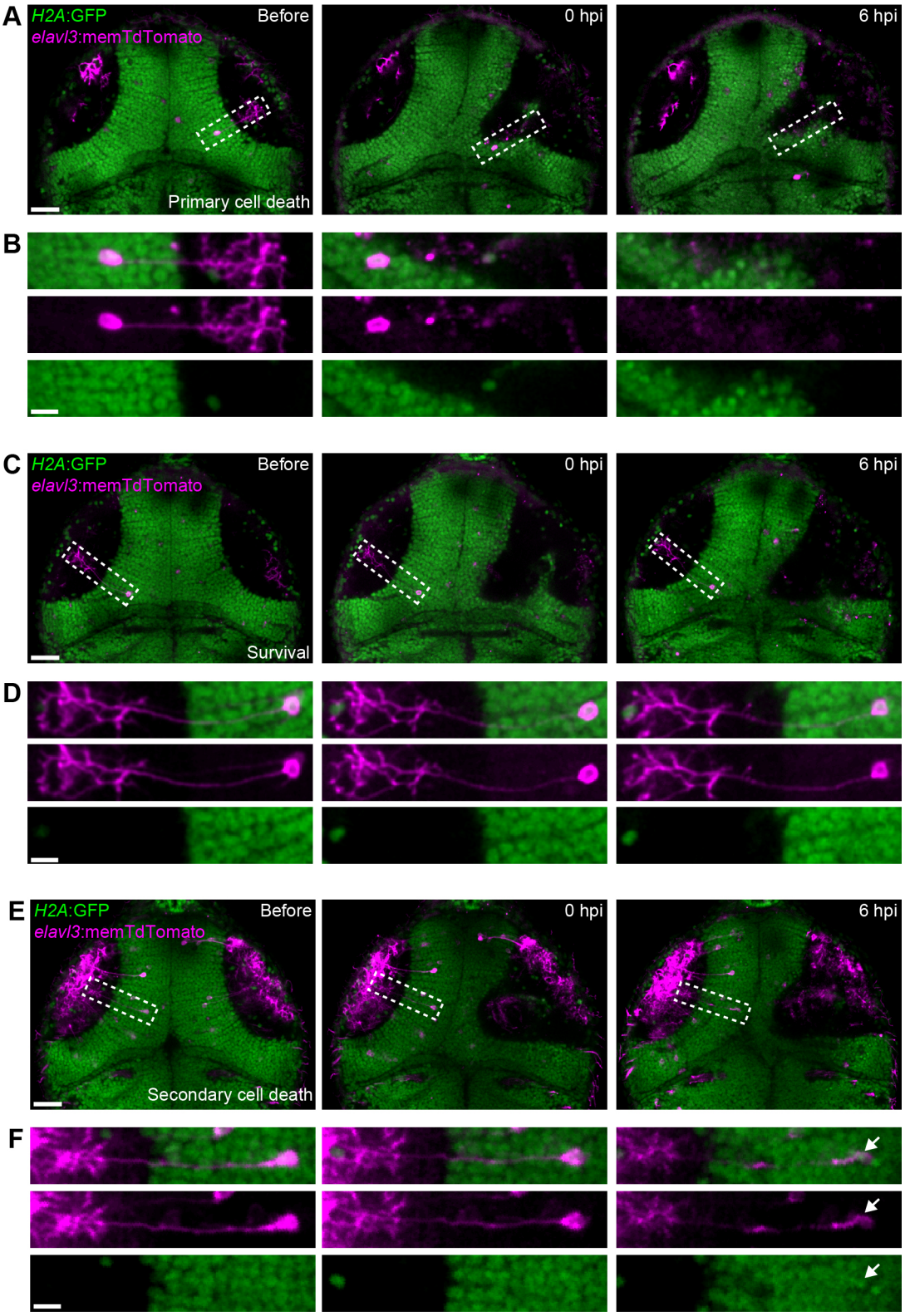

Fig. S3. *In vivo* imaging of individual tectal neurons shows that both primary and secondary cell death occur after brain injury. (A,C,E) Confocal images of the optic tectum of *H2A*:GFP transgenic animals, where tectal neurons labelled through injection of *elavl3*:memTdTomato plasmid DNA die through primary cell death (A), survive (C), or die through secondary cell death (E) after mechanical injury. Scale bars, 50 µm. (B,D,F) Close-up of neurons indicated in (A), (C) and (E). White arrow indicates pyknotic nucleus. Scale bars, 10 µm.

Figure S4

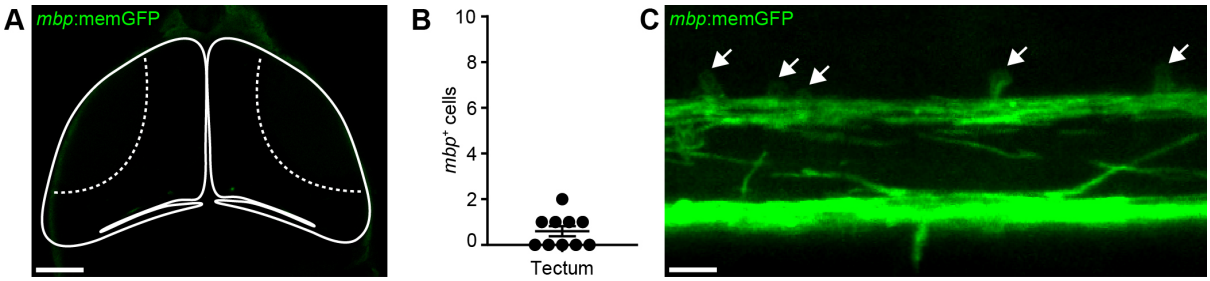

Figure S4. Very few oligodendrocytes reside in the optic tectum at 4 dpf. (A) Confocal image of the optic tectum of a *mbp*:memGFP animal. Scale bar, 50 µm. (B) Quantification of *mpb*$^{+}$ oligodendrocytes in the optic tectum. n = 10 animals. (C) Confocal image of the trunk region of a *mbp*:memGFP animal. White arrows indicate cell bodies of individual oligodendrocytes. Scale bar, 10 µm.

Figure S5

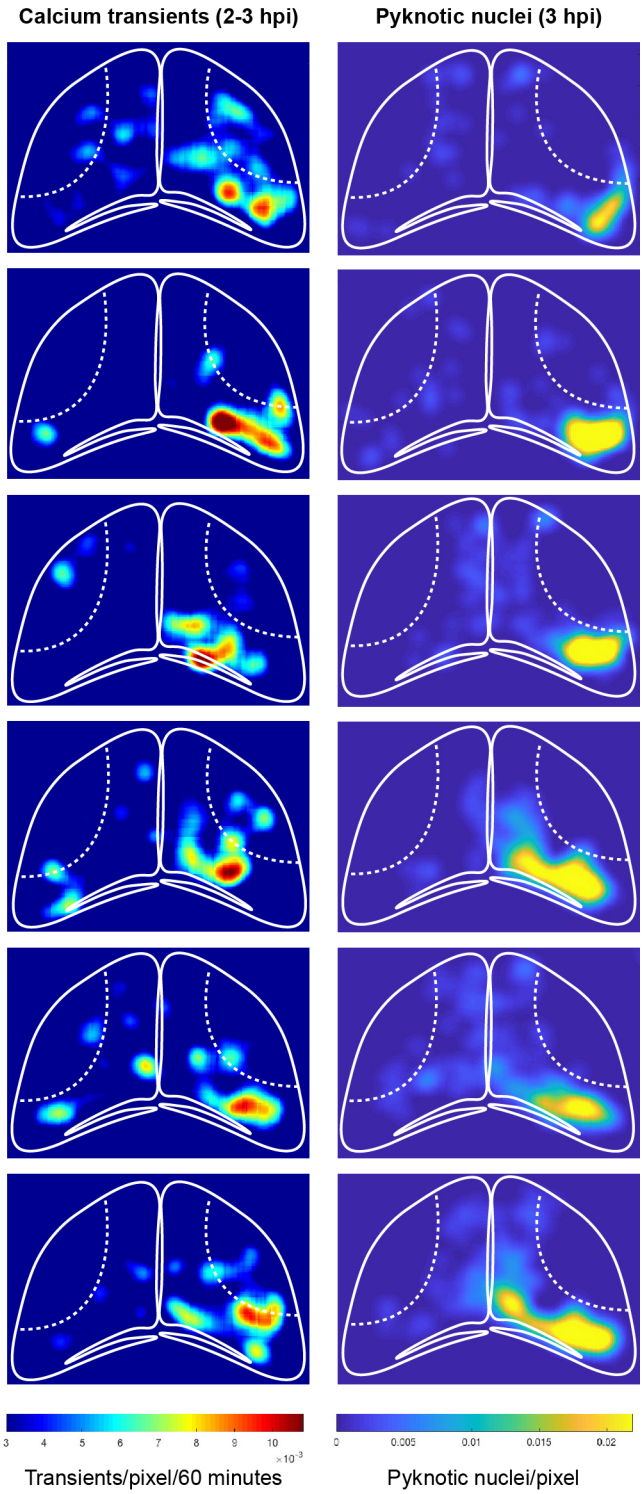

Fig. S5. The spatial pattern of calcium transients correlates with regions of cell death. Heat maps illustrating the spatial distribution of calcium transients occurring between 2 and 3 hpi (left), and of pyknotic nuclei at 3 hpi (right), in the same animals.

Figure S6

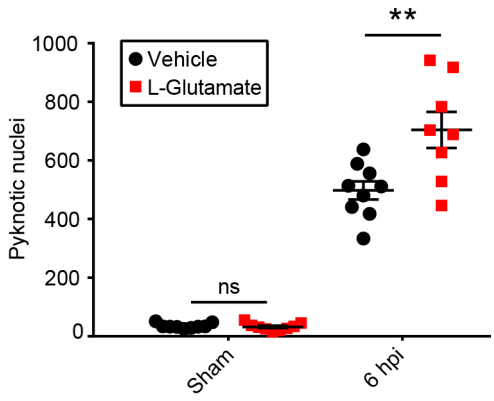

Fig. S6. L-Glutamate exacerbates secondary cell death after brain injury. Quantification of pyknotic nuclei in control animals or animals treated with L-Glutamate. n ≥ 8 animals per experimental group. ns, not significant and **, $p < 0.01$ in two-way ANOVA.

Figure S7

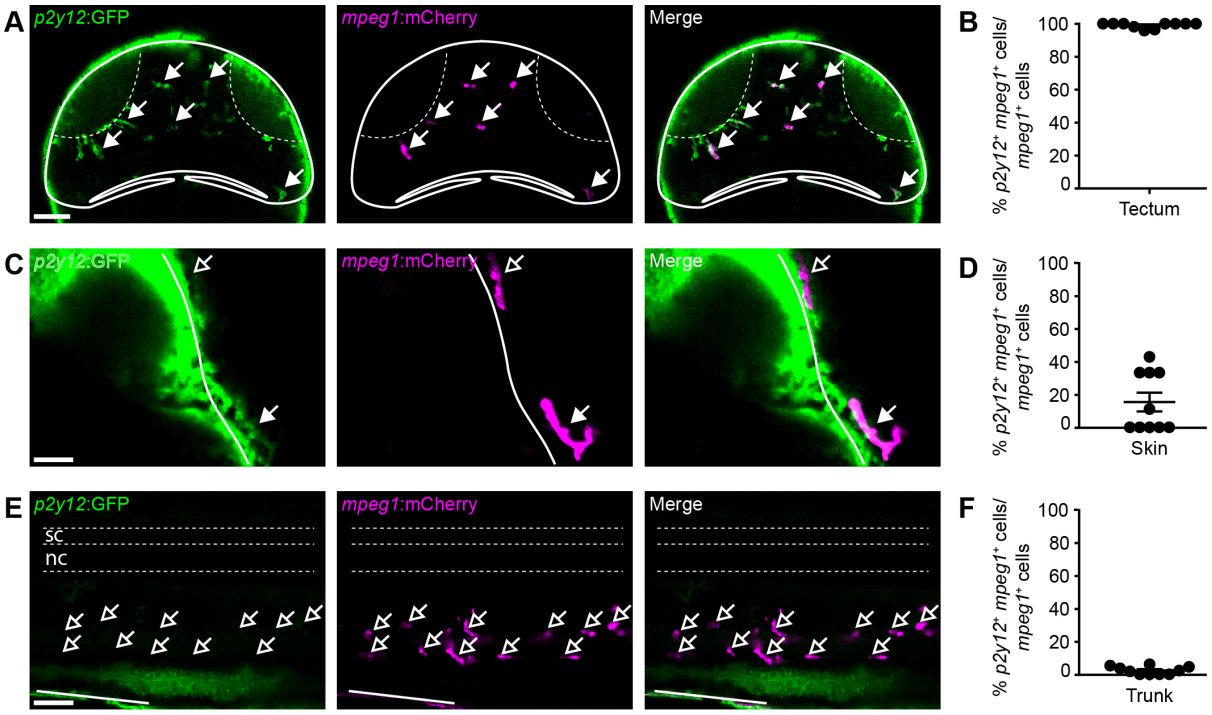

Figure S7. P2Y12 is expressed in virtually all *mpeg1*$^{+}$ tectal cells and some *mpeg1*$^{+}$ skin cells, but not in *mpeg1*$^{+}$ cells in the trunk. (A,C,E) Confocal images of the optic tectum (A), skin (C), and trunk (E) of a *p2y12*:GFP;*mpeg1*:mCherry animal. Filled or empty arrows indicate colocalisation, or lack thereof, between *p2y12* and *mpeg1*. Scale bars, 50 µm (A,E) and 20 µm (C). (B,D,F) Quantification of the proportion of *p2y12*$^{+}$/*mpeg1*$^{+}$ cells among all *mpeg1*$^{+}$ cells in the tectum (B), skin (D) and trunk (F). n = 10 animals per experimental group.

Figure S8

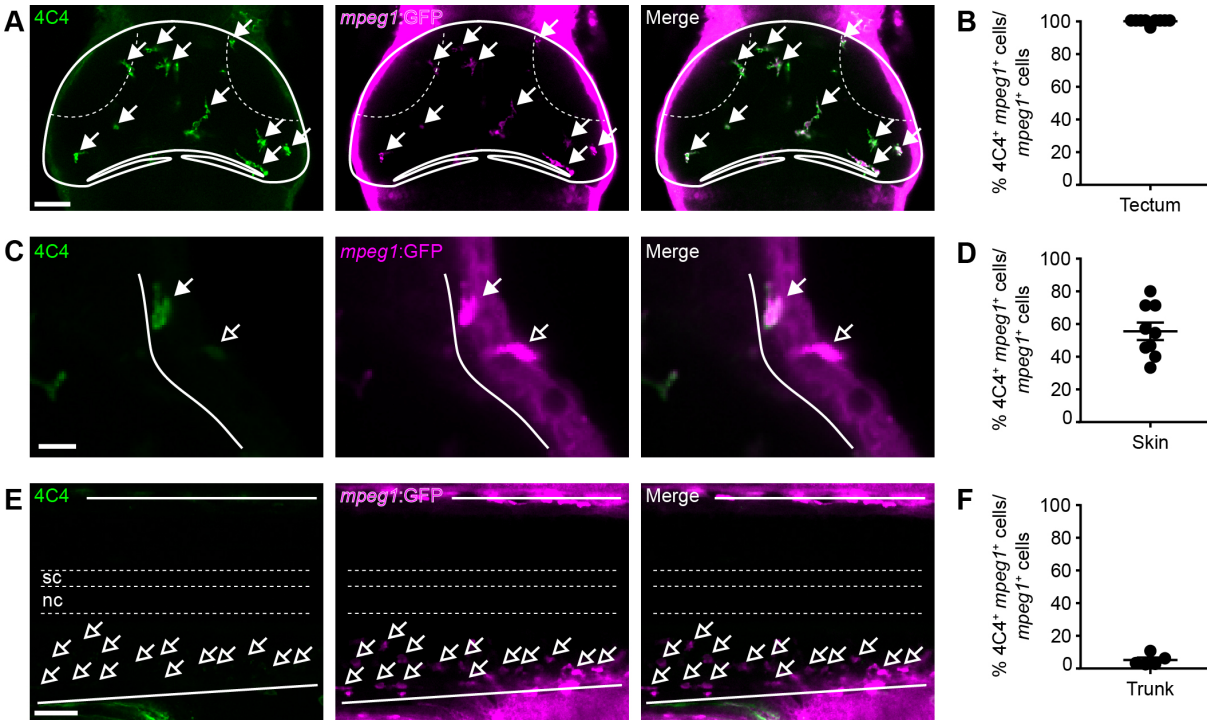

Figure S8. 4C4 immunohistochemistry labels virtually all *mpeg1*$^+$ tectal cells and some *mpeg1*$^+$ skin cells, but not *mpeg1*$^+$ cells in the trunk. (A,C,E) Confocal images of the optic tectum (A), skin (C) and trunk (E) of a *mpeg1*:GFP animal after 4C4 and GFP immunohistochemistry. Filled or empty arrows indicate colocalisation, or lack thereof, between 4C4 and *mpeg1*. Scale bars, 50 µm (A,E) and 20 µm (C). (B,D,F) Quantification of the proportion of 4C4$^+$/*mpeg1*$^+$ cells among all *mpeg1*$^+$ cells in the tectum (B), skin (D) and trunk (F). n ≥ 5 animals per experimental group.

Figure S9

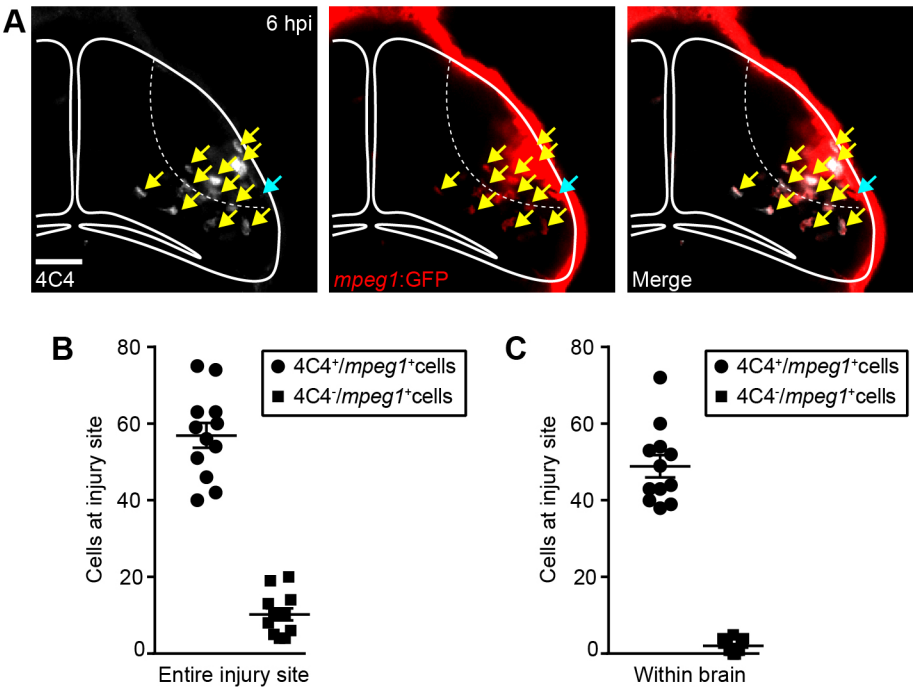

Fig. S9. The majority of *mpeg1*$^{+}$ cells at the injury site within the brain are also labelled by 4C4 immunohistochemistry. (A) Confocal images of the optic tectum at 6 hpi in *mpeg1*:GFP animals after 4C4 and GFP immunohistochemistry. Yellow arrows indicate 4C4^{+}/*mpeg1*$^{+}$ cells. Light blue arrow indicates a 4C4^{-}/*mpeg1*$^{+}$ cell. Scale bar, 40 µm. (B,C) Quantification of 4C4^{+}/*mpeg1*$^{+}$ and 4C4^{-}/*mpeg1*$^{+}$ cells at the entire injury site (B) or within the brain (C) at 6 hpi. n = 12 animals.

Figure S10

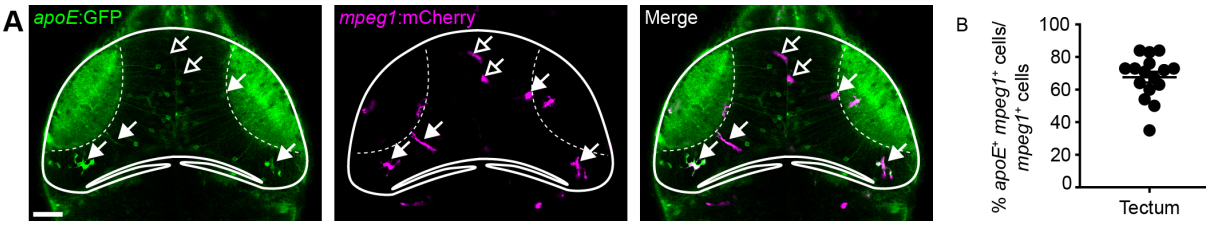

Figure S10. ApoE is expressed in a subset of *mpeg1*$^{+}$ tectal cells. (A) Confocal images of the optic tectum of an *apoE*:GFP;*mpeg1*:mCherry animal. Filled or empty arrows indicate colocalisation, or lack thereof, between *apoE* and *mpeg1*. Scale bar, 50 µm. (B) Quantification of the proportion of *apoE*$^{+}$/*mpeg1*$^{+}$ cells among all *mpeg1*$^{+}$ cells in the tectum. n = 16 animals.

Figure S11

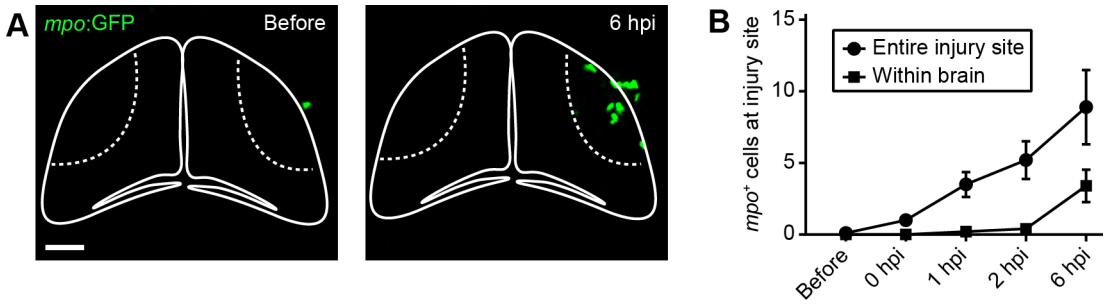

Fig. S11. Neutrophils are recruited to the injury site, but only a few are found within the brain. (A) Live imaging of the neutrophil reporter line *mpo*:GFP before injury and at 6 hpi. Scale bar, 50 µm. (B) Quantification of *mpo*$^{+}$ cells at the entire injury site and within the brain. n = 10 animals per experimental group.

Figure S12

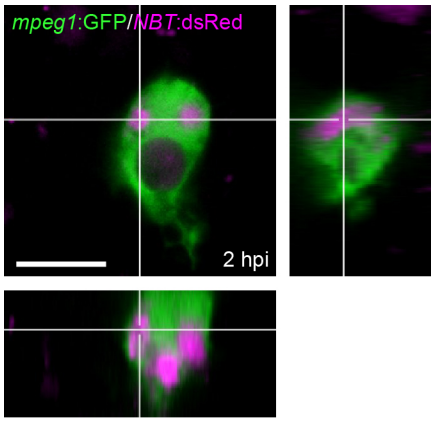

Fig. S12. Microglia take up substantial amounts of neuronal debris after brain injury. Orthogonal view of a microglial cell at 2 hpi in a *mpeg1*:GFP;*NBT*:dsRed animal. Scale bar, 10 µm.

Figure S13

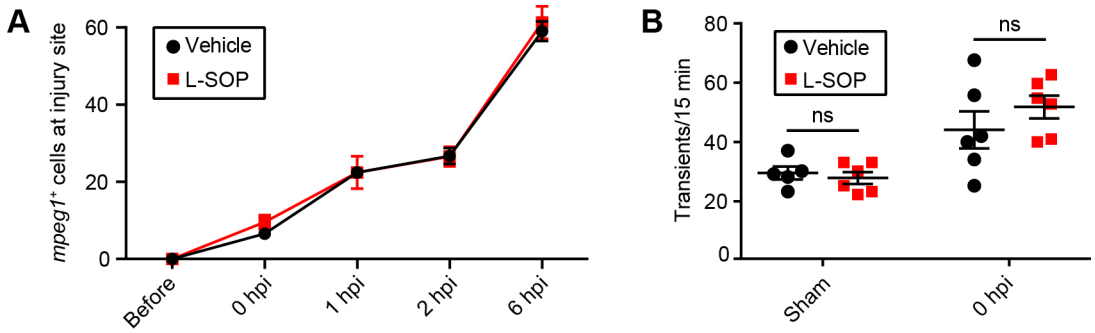

Fig. S13. L-SOP does not change microglial recruitment or tectal calcium dynamics. (A) Quantification of *mpeg1*$^{+}$ cells at the injury site within the brain in *mpeg1*:GFP animals treated with vehicle or L-SOP. n = 7 animals per experimental group. (B) Quantification of calcium transients by time-lapse imaging of *β-actin*:GCaMP6f larvae treated with vehicle or L-SOP. n ≥ 5 animals per experimental group. ns, not significant in two-way ANOVA.

Figure S14

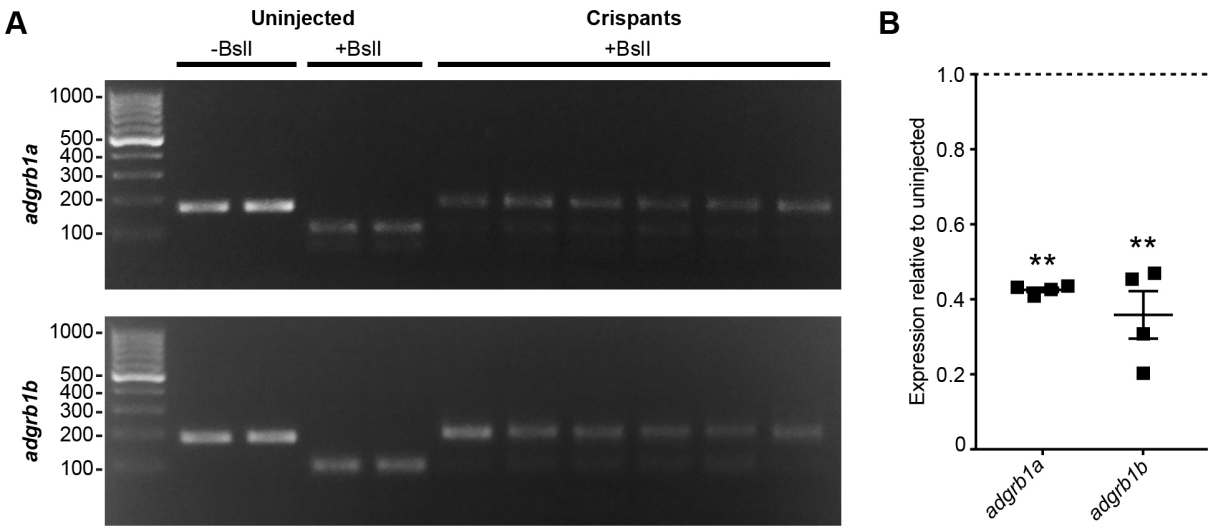

Fig. S14. CRISPR/Cas9-mediated gene editing reduces expression of the phosphatidylserine receptors *adgrb1a* and *adgrb1b*. (A) Restriction fragment length polymorphism analysis of the efficiency of CRISPR/Cas9-mediated gene editing of *adgrb1a* and *adgrb1b* in gRNA-injected F0 embryos. This demonstrates efficient somatic mutation of the gRNA target site, which becomes resistant to BslI restriction endonuclease digestion. One embryo was analysed per well. (B) RT-qPCR for *adgrb1a* and *adgrb1b* in gRNA-injected F0 embryos. Each data point represents one biological replicate, with mRNA from 10 animals pooled for each replicate. **, $p < 0.01$ in two-way ANOVA.

Figure S15

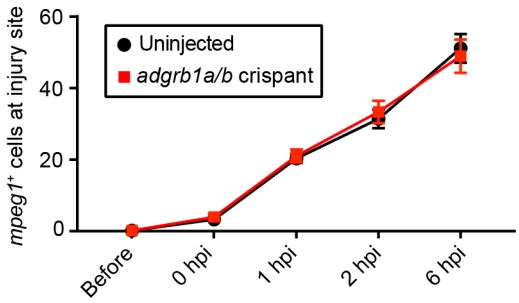

Fig. S15. Microglial recruitment is unchanged in *adgrb1a/b* crispants. Quantification of *mpeg1*$^{+}$ cells at the injury site within the brain in *adgrb1a/b* crispants as compared to uninjected *mpeg1*:GFP animals. n ≥ 9 animals per experimental group.

Figure S16

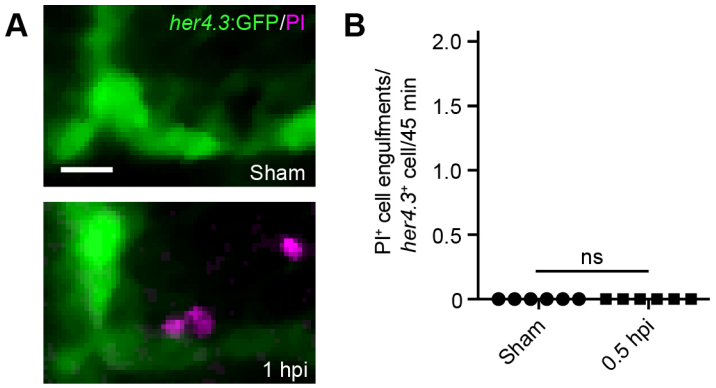

Fig. S16. *Her4.3*$^{+}$ radial glial cells do not make a major contribution to debris clearance after brain injury. (A) Confocal images of radial glial cells in *her4.3*:GFP animals before injury or at 1 hpi. Scale bar, 20 µm. (B) Quantification of phagocytosis of PI^{+} cells per radial glial cell from 30 to 75 min after injury. n = 6 animals per experimental group. ns, not significant in Mann-Whitney test.

Table S1. List of mutations after CRISPR/Cas9 editing of *adgrb1a*

Mutations in 37 out of 68 sequenced alleles (54% mutation rate)

GTGACCCACGCAATGCTGTTGCTCCACAAGGGGGGGCTGCTGGATATATGCTTTAGTGCCCGACTGCCTG	Wild type		x31
GTGACCCACGCAATGCTGTTGCTCCACAAtaccacagcatttaaatgctacaaatactctagccaag[…]	+341	(-2,+343)	
[…]cagtctgcctgtggagtactggagtcagtttatgataagcgaccacgaccatgctcgcaatgat[…]	+114	(-125, +239)	
GTGACCCACGCAATGCTGTTGCTCCACAAcataaaaacattgtggatatatatGGGGCTGCTGGATATAT	+20	(-3, +23)	
GTGACCCACGCAATGCTGTTGCTCCACAggatatatgctttagtgcccgaCTGCTGGATATATGCTTTAG	+14	(-8, +22)	
GTGACCCACGCAATGCTGTTGCTCCACgcaatgctgttgcttGGGGGGGCTGCTGGATATATGCTTTAGT	+13	(-2, +15)	
GTGACCCACGCAATGCTGTTGCTCCACAAGGGGGGcatatatccaCTGCTGGATATATGCTTTAGTGCCC	+9	(-1, +10)	
GTGACCCACGCAATGCTGTTGCTCCACAgctccacaggggGGCTGCTGGATATATGCTTTAGTGCCCGAC	+6	(-6, +12)	
GTGACCCACGCAATGCTGTTGCTCCACAActgctGGGGGGGCTGCTGGATATATGCTTTAGTGCCCGACT	+5		
GTGACCCACGCAATGCTGTTGCTCCACAActggatatatgCTGCTGGATATATGCTTTAGTGCCCGACTG	+4	(-7, +11)	
GTGACCCACGCAATGCTGTTGCTCCACgcaatgctGGGGCTGCTGGATATATGCTTTAGTGCCCGACTGC	+3	(-5, +8)	
GTGACCCACGCAATGCTGTTGCTCCACAAacgtatGGGGCTGCTGGATATATGCTTTAGTGCCCGACTGC	+3	(-3, +6)	
GTGACCCACGCAATGCTGTTGCcccacagcaGGGGGGCTGCTGGATATATGCTTTAGTGCCCGACTGCCT	+1	(-8, +9)	
GTGACCCACGCAATGCTGTTGCTCCACAAcagcatGGCTGCTGGATATATGCTTTAGTGCCCGACTGCCT	+1	(-5, +6)	
GTGACCCACGCAATGCTGTTGCTCCACAACAGGGGGCTGCTGGATATATGCTTTAGTGCCCGACTGCCTG	*2		x3
GTGACCCACGCAGTGCTGTTGCTCCACAAGGGGGGGCTGCTGGACATATGCTTTAGTGCCCGACTGCCTG	*1		
GTGACCCACGCAATGCTGTTGCTCCACA-tatatGCTGCTGGATATATGCTTTAGTGCCCGACTGCCTGC	-1	(-7, +6)	
GTGACCCACGCAATGCTGTTGCTCCA-atgctGGGGCTGCTGGATATATGCTTTAGTGCCCGACTGCTTG	-1	(-6, +5)	
GTGACCCACGCAATGCTGTTGCTCCACA-GGGGGGGCTGCTGGATATATGCTTTAGTGCCCGACTGCCTG	-1		
GTGACCCACGCAATGCTGTTGCTCCACA--tatatGCTGCTGGATATATGCTTTAGTGCCCGACTGCCTG	-2	(-2, +5)	
GTGACCCACGCAATGCTGTTGCTCCACA--GGGGGGCTGCTGGATATATGCTTTAGTGCCCGACTGCCTG	-2		
GTGACCCACGCAATGCTGTTGCTCCACA---gggggtTGCTGGATATATGCTTTAGTGCCCGACTGCCTG	-3	(-9, +6)	
GTGACCCACGCAATGCTGTTGCTCCtt---GGGGGGCTGCTGGATATATGCTTTAGTGCCCGACTGCCTG	-3	(-5, +2)	x2
GTGACCCACGCAATGCTGTTGCTCCACA---GGGGGCTGCTGGATATATGCTTTAGTGCCCGACTGCCTG	-3		
GTGACCCACGCAATGCTGTTGCTCCA----tatatgCTGCTGGATATATGCTTTAGTGCCCGACTGCCTG	-4	(-10, +6)	
GTGACCCACGCAATGCTGTTGCTCCACAA----tGGCTGCTGGATATATGCTTTAGTGCCCGACTGCCTG	-4	(-5, +1)	
GTGACCCACGCAATGCTG-----gatatgctGGGGGCTGCTGGATATATGCTTTAGTGCCCGACTGCCTG	-5	(-13, +8)	
GTGACCCACGCAATGCTGTTGCTCC-----gcaatGCTGCTGGATATATGCTTTAGTGCCCGACTGCCTG	-5	(-10, +5)	x3
GTGACCCACGCAATGCTGTTGCTCCACAA-----tGCTGCTGGATATATGCTTTAGTGCCCGACTGCCTG	-5	(-6, +1)	
GTGACCCACGCAATGCTGTT---------GGGGGGGCTGCTGGATATATGCTTTAGTGCCCGACTGCCTG	-9		
GTGACCCACGCAATGCTGTTGCTCCAC----------GCTGGATATATGCTTTAGTGCCCGACTGCCTG	-11		
GTGACCCACGCAATGCTG----------GGGCTGCTGGATATATGCTTTAGTGCCCGACTGCCTG	-15		
GTGACCCACGCAAT----------GGGGGGCTGCTGGATATATGCTTTAGTGCCCGACTGCCTG	-16		
GTGACCCACGCAATGCTG----------CTGCTGGATATATGCTTTAGTGCCCGACTGCCTG	-18		
GTGACCCACGCAATGCT----------accGGATATATGCTTTAGTGCCCGACTGCCTG	-21	(-24, +3)	

The gRNA target site is underlined. Inserted bases are highlighted in grey, and changed bases are highlighted in green.

Table S2. List of mutations after CRISPR/Cas9 editing of *adgrb1b*

Mutations in 42 out of 45 sequenced alleles (93% mutation rate)

CGACTCAGAGAACCCGCGAGTGTAACGGACCCTCATACGGCGGCTCCGAGTGCAGAGGGGAATGGCTGGA	wild type		x3
CGACTCAGAGAACCCGCGAGTGTAACGGACCCTaaccctaaccctaaccctaaccctaaccctaaccctaacc[…]	+88	(-3, +91)	
CGACTCAGAGAACCCGCGAGTGTAACGGACCCTCAgtggggaatggctggagCGGCGGCTCCGAGTGCAG	+15	(-2, +17)	
CGACTCAGAGAACCCGCGAGTGTAACGGACCCTCtgccntggTACGGCGGCTCCGAGTGCAGAGGGGAAT	+7	(-1, +8)	
CGACTCAGAGAACtcgcgggtgtaacggatcctcattcatcCGGCGGCTCCGAGTGCAGAGGGGAATGGC	+4	(-24, +28)	
CGACTCAGAGAACCCGCGAGTGTAACGGACCCTCATtcatcCGGCGGCTCCGAGTGCAGAGGGGAATGGC	+4	(-1, +5)	x2
CGACTCAGAGAACCCGCGAGTGTAACGGACCgagtgcagagGGCGGCTCCGAGTGCAGAGGGGAATGGCT	+3	(-7, +10)	
CGACTCAGAGAACCCGCGAGTGTAACGGACCCTCAtTACGGCGGCTCCGAGTGCAGAGGGGAATGGCTGG	+1		x2
CGACTCAGAGAACCCGCGAGTGTAACGGACCCTCA gtGGCGGCTCCGAGTGCAGAGGGGAATGGCTGGA	-1	(-3, +2)	
CGACTCAGAGAACCCGCGAGTGTA gcggaccccTACGGCGGCTCCGAGTGCAGAGGGGAATGGCTGGA	-2	(-11, +9)	
CGACTCAGAGAACCCGCGAGTGTAACGGACCCTC ACGGCGGCTCCGAGTGCAGAGGGGAATGGCTGGA	-2		
CGACTCAGAGAACCCGCGAGTGTAACGG gccgTACGGCGGCTCCGAGTGCAGAGGGGAATGGCTGGA	-3	(-7,+4)	
CGACTCAGAGAACCCGCGAGTGTAACGGACCC TACGGCGGCTCCGAGTGCAGAGGGGAATGGCTGGA	-3		
CGACTCAGAGAACCCGCGAGTGTAACGGACCCTCA gaCTCCGAGTGCAGAGGGGAATGGCTGGA	-6	(-8, +2)	
CGACTCAGAGAACCCGCGAGTGTAACGGACCCTCA atcatTCCGAGTGCAGAGGGGAATGGCTGGA	-4	(-9, +5)	x2
CGACTCAGAGAACCCGCGAGTGTAACGGACCCT CGGCGGCTCCGAGTGCAGAGGGGAATGGCTGGA	-4		x5
CGACTCAGAGAACCCGCGAGTGTAACGGACCga GGCTCCGAGTGCAGAGGGGAATGGCTGGA	-8	(-10, +2)	
CGACTCAGAGAACCCGCGAGTGTAACGGACC GGCTCCGAGTGCAGAGGGGAATGGCTGGA	-10		
CGACTCAGAGAACCCGCGAGTGTAAC taGCGGCTCCGAGTGCAGAGGGGAATGGCTGGA	-11	(-13, +2)	
CGACTCAGAGAACCCGCGAGTGTAACGGACCC TCCGAGTGCAGAGGGGAATGGCTGGA	-12		x5
CGACTCAGAGAACCCGCGAGTGTA cggcgaCTCCGAGTGCAGAGGGGAATGGCTGGA	-13	(-19, +6)	
CGACTCAGAGAACCCGCGAGTGT ACGGCGGCTCCGAGTGCAGAGGGGAATGGCTGGA	-13		
CGACTCAGAGAACCCGCGAGTGTAACGGAC CCGAGTGCAGAGGGGAATGGCTGGA	-15		x4
CGACTCAGAGAACCCG agTACGGCGGCTCCGAGTGCAGAGGGGAATGGCTGGA	-17	(-19, +2)	x2
CGA CTCCGAGTGCAGAGGGGAATGGCTGGA	-40		
C CTCCGAGTGCAGAGGGGAATGGCTGGA	-42		
[…] […]	-98	(-135, +37)	

The gRNA target site is underlined. Inserted bases are highlighted in grey.

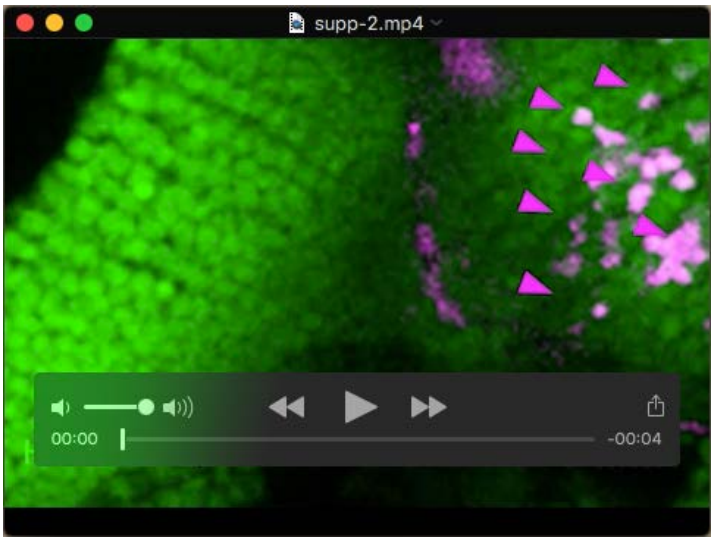

Movie 1. *In vivo* time-lapse imaging shows clearance of PI$^+$ cells and appearance of pyknotic nuclei after brain injury. The movie was recorded in an *H2A*:GFP animal in the presence of PI from 120 to 230 min after injury. PI$^+$ cells (magenta arrows) are removed, while pyknotic nuclei (white arrows) progressively appear within this time window. Scale bar, 15 µm.

Movie 2. Macrophage-lineage cells display limited baseline motility in sham animals. The movie shows maximum intensity projections of z-stacks of the optic tectum in a sham *mpeg1*:GFP animal, indicating limited movement of the cell bodies of macrophage-lineage cells. The traces indicate cell body displacement of individual cells over 25 min. Scale bar, 40 µm.

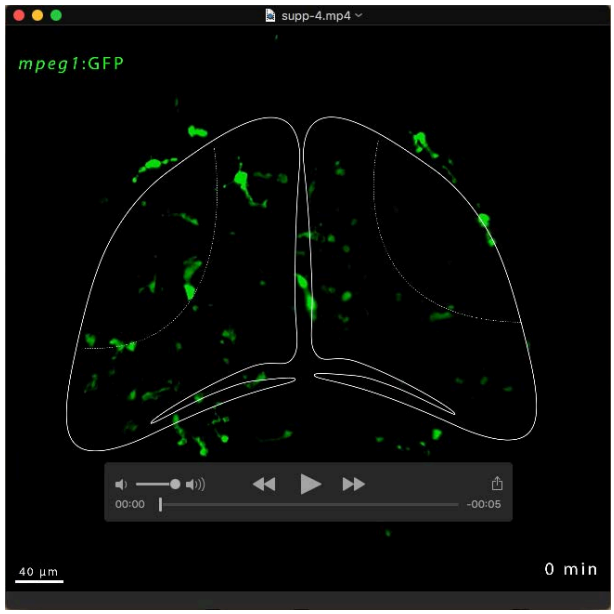

Movie 3. After injury, macrophage-lineage cells rapidly migrate towards the site of brain injury. The movie shows maximum intensity projections of z-stacks of the optic tectum in an injured *mpeg1*:GFP animal, revealing rapid directional movement of macrophage-lineage cells towards the lesion site after brain injury. The traces indicate cell body displacement of individual cells in the 140 min following injury. Scale bar, 40 µm.

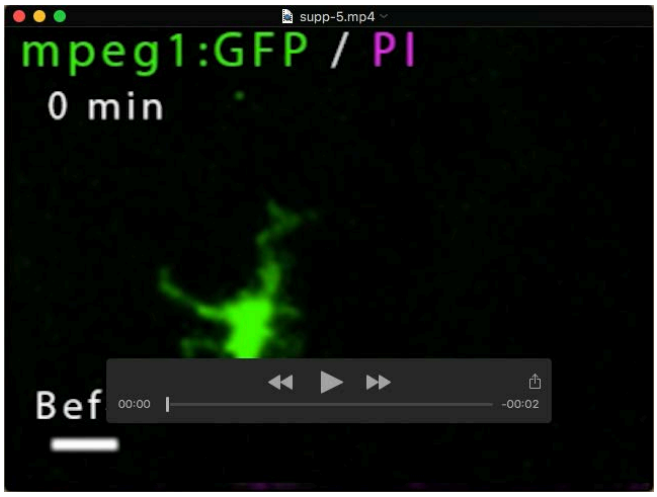

Movie 4. Microglia actively survey their environment in sham animals. Time-lapse imaging of a microglial cell reveals the highly dynamic processes with which it monitors its environment over 30 min in a sham *mpeg1*:GFP animal. Scale bar, 15 µm.

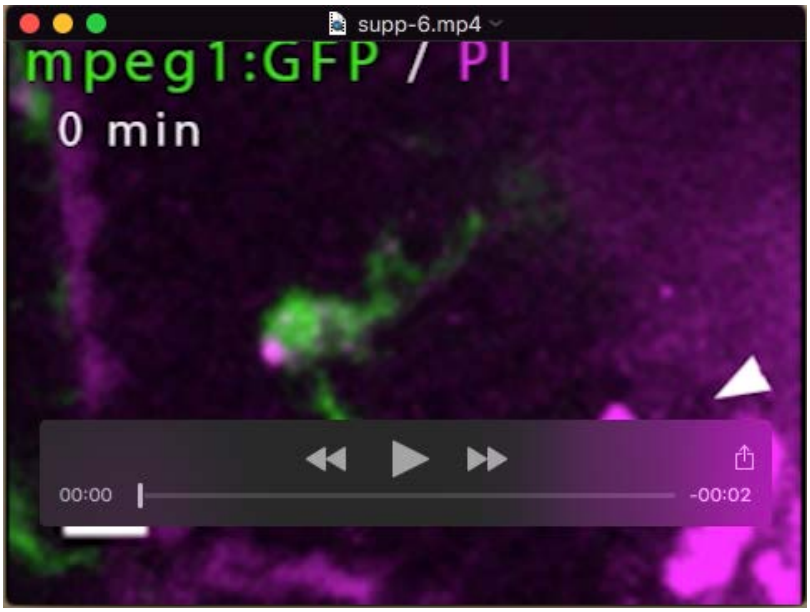

Movie 5. Microglia rapidly engulf PI$^+$ cells after brain injury. Time-lapse imaging shows a microglial cell as it approaches and engulfs a PI$^+$ cell after tectal injury in a *mpeg1*:GFP animal. The movie was recorded from 30 to 66 min following injury. Scale bar, 15 μm.

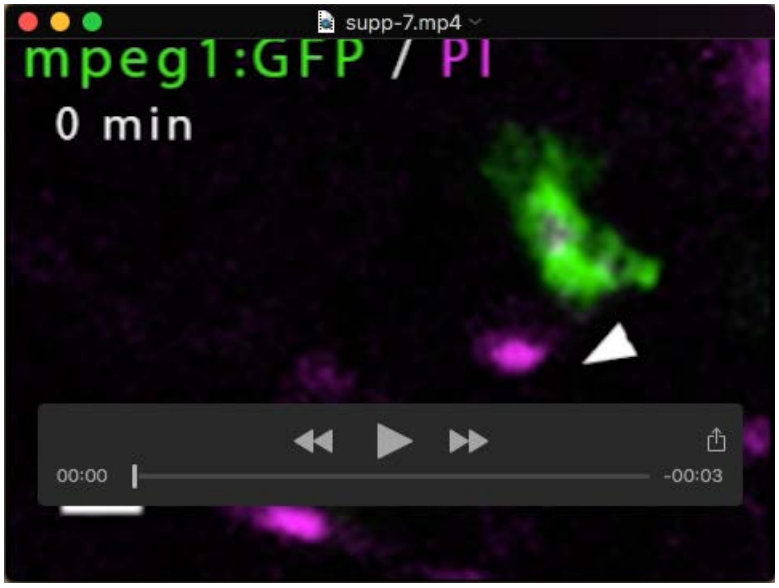

Movie 6. Microglial phagocytosis is reduced in animals treated with L-SOP. Time-lapse imaging of a microglial cell in a *mpeg1*:GFP animal treated with L-SOP. The microglial cell approaches a PI$^+$ cell, but does not engulf it. The movie was recorded from 30 to 72 min following injury. Scale bar, 15 μm.

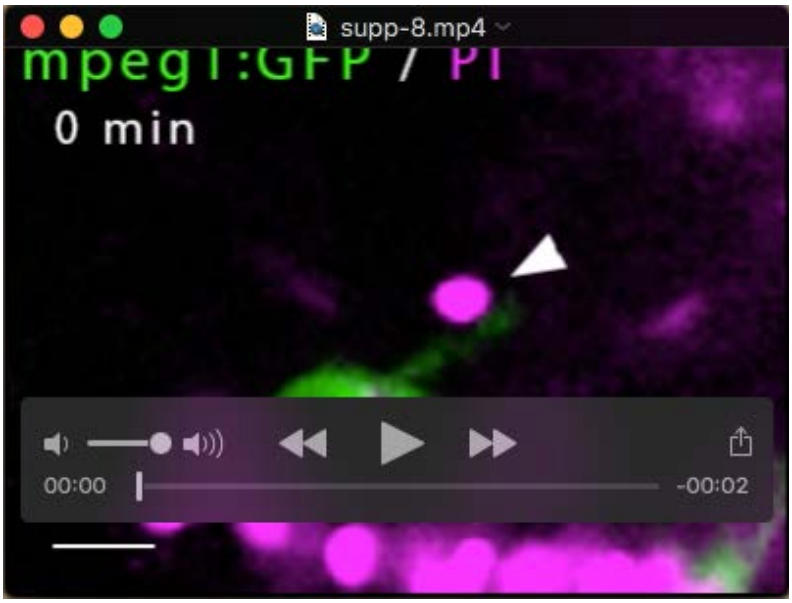

Movie 7. Microglial uptake of cellular debris is reduced in *adgrb1a/b* crispants. In a *mpeg1*:GFP animal injected with *adgrb1a/b* gRNAs, a microglial cell extends a process towards a PI^+ cell but does not proceed to phagocytose it. The movie was recorded from 30 to 66 min following injury. Scale bar, 15 μm.